FLUCTUATION OF RIP CURRENT MEASURED IN SHALLOW WATER REGION WITH SMALL TIDAL RANGE

Ichiro Deguchi[1], Mamoru Arita[2] and Takumi Yoshii[3]

Disappearance and formation processes of rip channel are discussed based on the field measurements of wave height, current velocity, bottom topography and flow pattern of near-shore current. Sudden increase in wave height together with the change in the wave direction took place during a half day caused these phenomena and rip current rose and fell according to the transition of the bottom topography. Furthermore, flow pattern of rip current was not steady but transformed itself with low frequency fluctuations of the period of few minutes. It is found that such low frequency fluctuations are caused by the intrinsic fluctuations of the incident waves (grouping waves) through the numerical simulations.

Keywords: rip channel; rip current; hot spot, numerical simulation

INTRODUCTION

Rip current in rip channel and/or embayment of a large (mega) cusp can be calculated as a steady flow by numerical simulations when a bottom profile and incident wave conditions are given with proper boundary conditions. However, the measured rip current is not always steady. Even under the conditions of steady incidence of constant waves, the magnitude of rip current is not steady due to the interaction between fluid motion and bottom topography. The authors have been conducting field observations of nearshore currents, incident waves and bottom topography with focus on the fluctuation of rip current of the time scale from few minutes to few hours since 2002. The latter time scale corresponds to the formation and annihilation of rip channel.

The purpose of this study is to show that the fluctuation with time scale few minutes is caused by the intrinsic fluctuation in incident waves and significant change in the incident wave took place during few hours is responsible for the generation and annihilation of rip channel through the interaction between wave transformation, wave-induced current and topography change based on the results of field observations in 2007 and 2009.

OVERVIEW OF OBJECTIVE BEACH

Field measurements were carried out at Uradome Beach in Tottori, Japan since 2002. The beach is a beautiful pocket beach of the length about 1.6km (Fig.1) and many people enjoy swimming in summer but three fatal accidents were caused by the rip current during these 6years. Two submerged breakwaters of the length 400m and the crown width 30m were constructed at the depth about 5m.

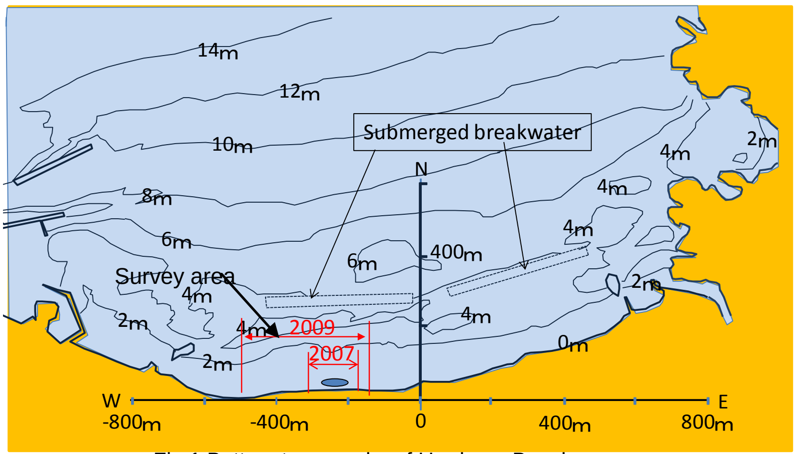

Fig.1 Bottom topography of Uradome Beach
(The contour lines are drawn based on the sounding in 2004)

[1] Department of Civil Engineering, Osaka University, Yamadaoka2-1, Suita, Osaka, 565-0871, Japan
[2] Department of Civil Engineering, Osaka University, Yamadaoka2-1, Suita, Osaka, 565-0871, Japan
[3] Environmental Science Research Lab., Central Research Institute of Electric Power Industry, Abiko 1646, Abiko, 270-2294Japan

The bottom slope is relatively gentle, about 1/50 near the shoreline and bed material is fine sand of the mean grain size about 0.02cm. The spring range of this beach is less than 30cm and we can neglect the effect of tide. The origin of the co-ordinate in the figure is the base point of our measurements.

Figure 2 shows the comparison of the locations of shoreline for these 6years measured by GPS surveys mentioned latter. Any correction of tidal level is not made. The shoreline configurations in eastern part of the beach are smooth. On the other hands, shoreline configurations in the western part are substantial and complex.

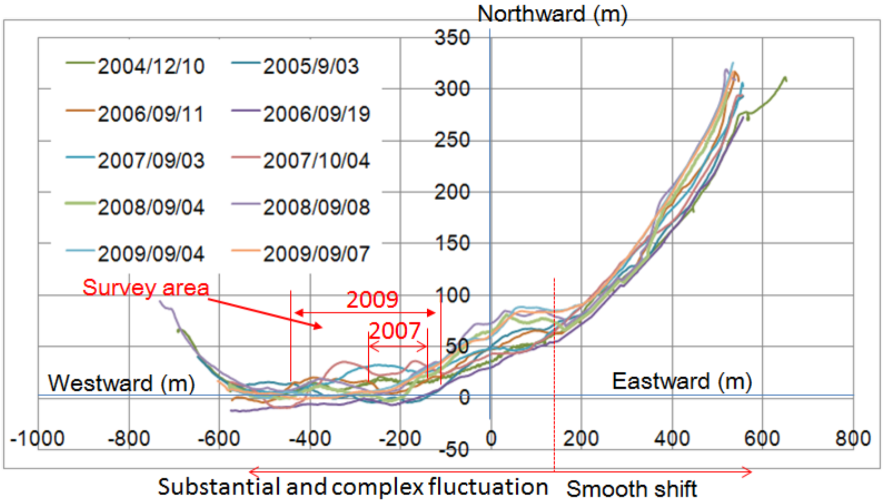

Fig.2 Comparison of the locations of shoreline for these 6years

The regions of the bathymetric surveys in 2007 and 2009 are shown in Figs.1 and 2. In 2007, rip channel already existed and rip current was generated on the channel. However, the channel disappeared according to the change in incident wave characteristics. In 2009, there was not any rip channel at first. The rip current was generated after the sudden increase in incident wave heights and the rip channel begun to form.

METHOD OF OBSERVATIONS

Surface displacement and water particle velocity

Surface displacement and water particle velocity around the rip current were measured by arrayed set of electro-magnetic current meter and pressure sensor as shown in Fig.3. In 2007, we put five sets of sensors along the center of the rip channel. In 2009, we put five sets of sensors at 5m interval on line where rip channel might be formed. Incident waves were measured by an ultrasonic wave gauge (Wave-hunter-Σ) set at the depth of 7-8m. Sampling frequency of the ultrasonic wave gauge was 2Hz and sampling frequency of EMC and the pressure sensor was 1Hz.

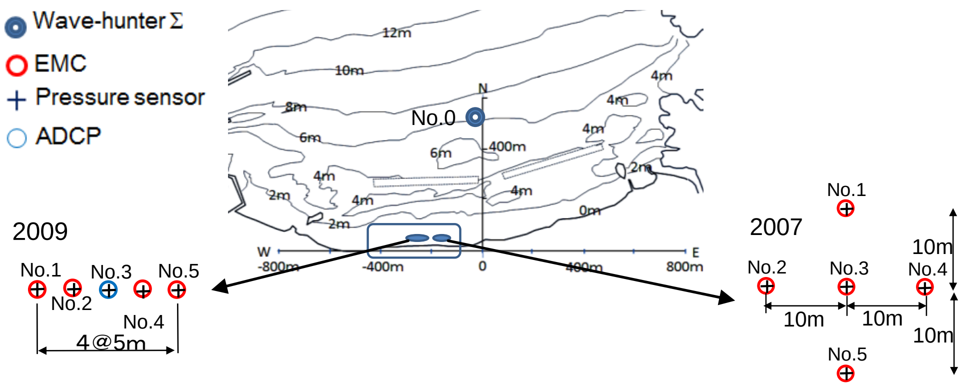

Fig.3 Arrangement of sensor array

Bottom Topography and Flow Pattern of Near Shore Current

We measured the bottom topography using a relative positioning system of D-GPS. Students wear GPS receivers on their back walk around the survey area. Figure 4 is an example of GPS trajectory. From this data, we made the water depth data at 0.5m grid as shown in Fig.5.

By this method we can measure bottom profile in the region shallower than 1.5m. In the region of the water depth deeper than 1.5m, we estimate the water depth using time averaged brightness of the images recorded on the video mounted on the balloon (Arita et al. 2007).

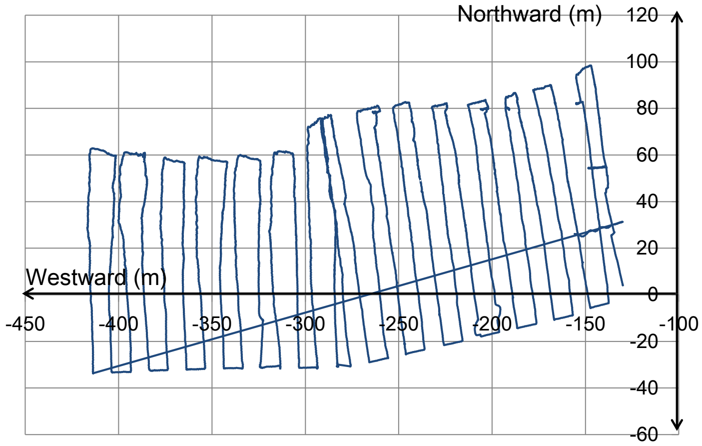

Fig.4 Example of trajectory of GPS receiver (2009,09.03)

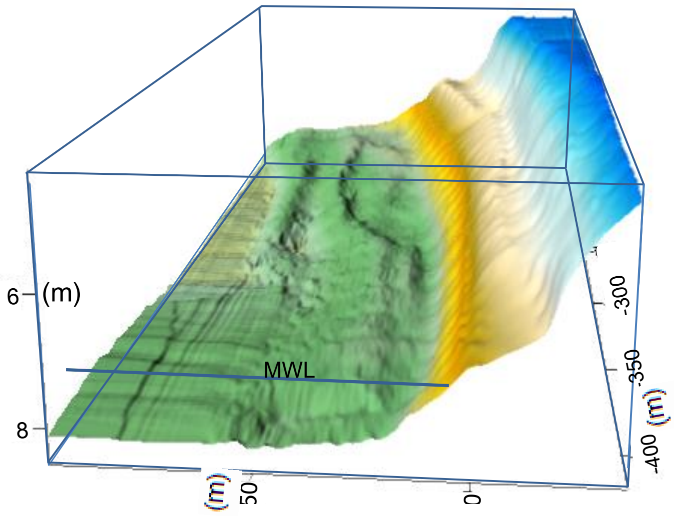

Fig.5 Estimated bottom profile of 0.5m mesh (2009,09.03)

Flow patterns of near-shore current were observed by a local remote sensing using balloon where a remotely operated video camera was installed (Deguchi et al., 2006). The balloon was usually moored about 120m to 150m above the sea surface.

FLUCTUATION OF NEARSHORE CURRENT OF THE TIME SCALE OF FEW MINUTES IN THE FADING PROCESS OF RIP CHANNEL (2007)

A clear rip channel existed when we started the field measurement in 2007. We put our sensor array along the rip channel on September 4. Intermittent but clear rip current with large fluctuations in current velocities and water surface displacements of the time scales of few minutes came up until September 5. In time, the places we put the sensors became shallow and the deepest part shifted to the west. Finally the rip channel disappeared on September 7.

Measured Bottom Topography in the Fading Process of Rip Channel

Figure 6 shows examples of measured bottom topography in 2007. It is found that there was clear rip channel in the bottom topography measured on Sept. 5 (Fig.(a)). The position of the sensors No.3 was located in the center of the channel. The deeper part moved westward about 20m in time and the rip channel disappeared around our sensor array on Sept. 7 (Fig.(c)).

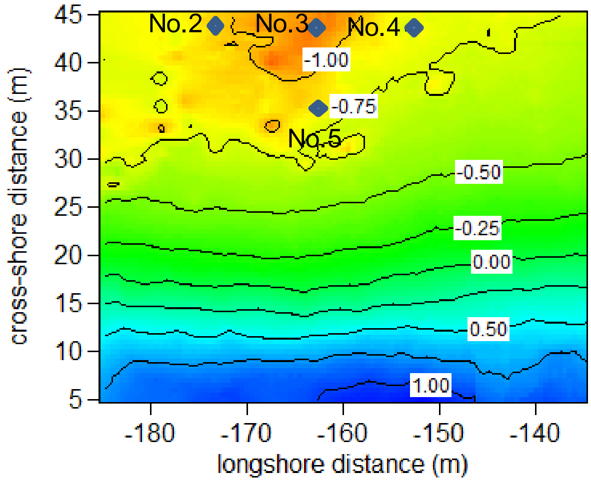

(a) September 5

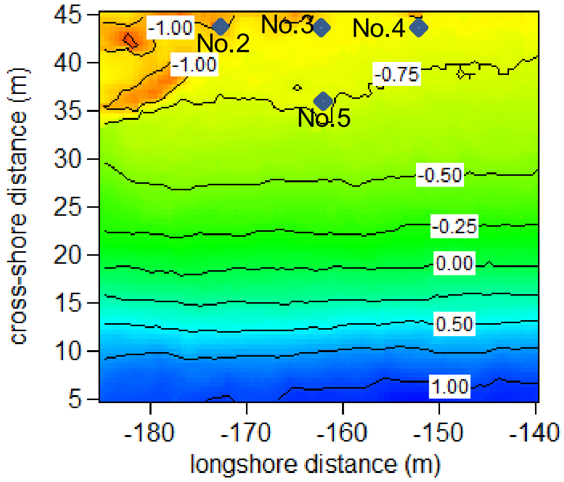

(b) September 6

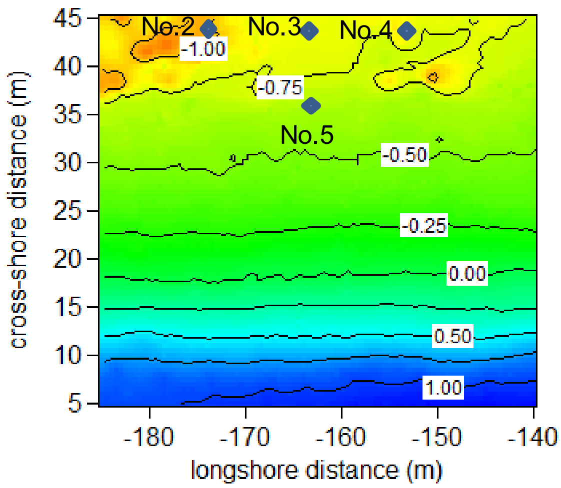

(c) September 7

Fig.6 Measured bottom topography in Sept. 2007

Incident Waves during Field Observation

During this time, relatively large waves due to Typhoon 200709 attacked the beach and we lost the ultrasonic wave gauge set at the depth about 8m. Therefore, we look into the incident wave characteristics using wave data measured off Tottori harbor (NOWPHAS, 2007) near the objective beach.

Figure 7 is the time history of incident wave height and period (Fig.(a)) and wave direction (Fig.(b)) during the field study. Incident wave height increased from 0.5m to 2.2m during September 4 and 6. The wave direction also changed from NNW to NNE 10deg. to 20deg. east from the north in the morning of Sept 4 and incident wave kept its direction until Sept. 6.

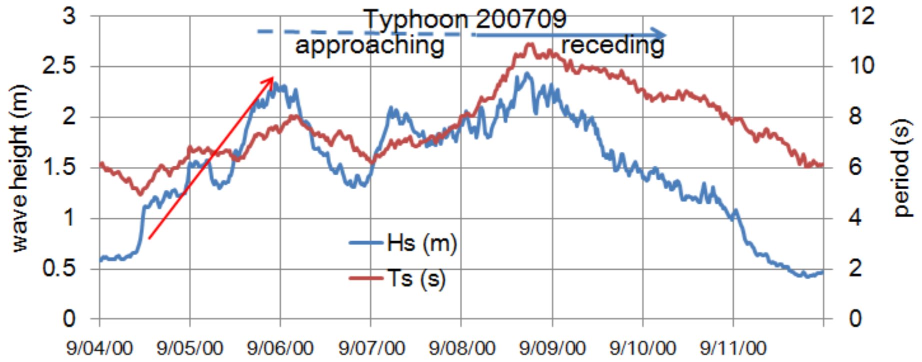

(a)Significant wave height and period

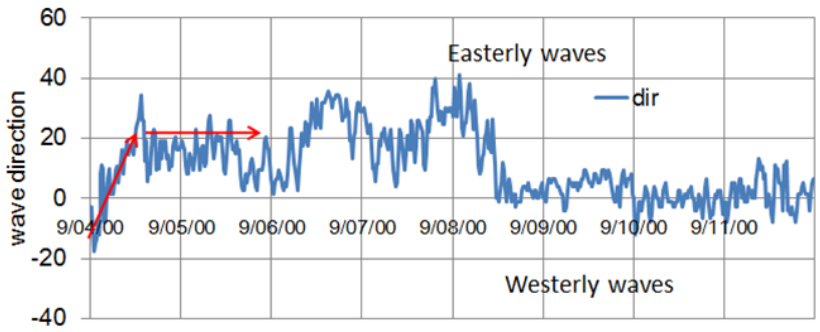

(b)Principle direction of incident waves

Fig.7 Incident wave characteristics of Sept. 2007 (NOWPHAS 2007)

Measured Wave Height and Current Velocity in Shallow Water Region

Figure 8 illustrates the one hour time averaged cross-shore component (Fig.(a)) and longshore component (Fig.(b)) of the measured current velocities. The digit in the legend symbol of the figure corresponds to the location of the sensor in the array and upper right figure in these figures illustrates the arrangement of sensor array.

Until noon of Sept. 5, mean current toward NNE occurred. After that, offshore component of the current decreased and westward longshore current stood out until the noon of Sept6. The averaged velocity of westward longshore current was about 0.4m/s. An abrupt change in the wave direction followed by the rapid increase in wave height generated this longshore current and the longshore current seems to wipe out the rip channel.

As can be seen from these figures, the mean current velocity measured at each sensor varies in a wide range. The maximum distance of the sensors was about 20m. This means that there was a large spatial gradient in the current filed.

It is also confirmed that clear low frequency fluctuations exist in the raw data of measured velocities and water surface displacement especially in Sept 5. Figure 9 shows an example of the measured raw velocity (cross-shore component) at No.1 sensor in the morning of Sept.5, 11:00-11:05. In the figure, 4s-moving averaged value is also shown. In this period, low frequency fluctuations of the period 60s can be seen.

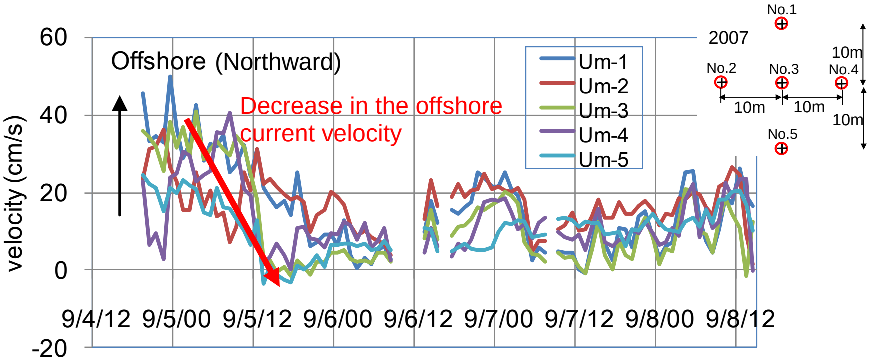

(a)cross-shore component

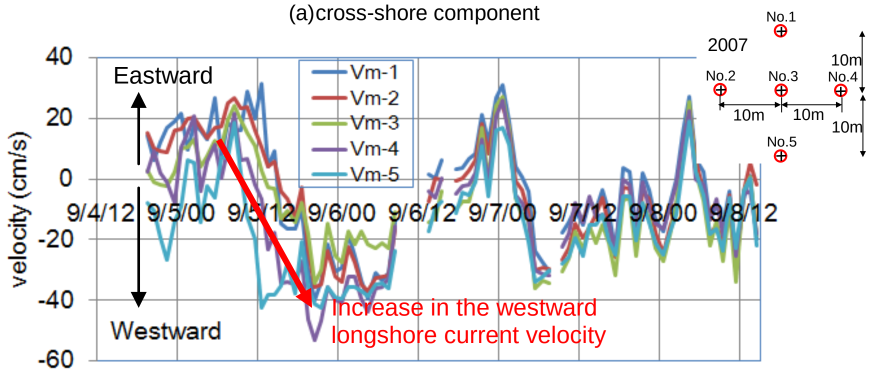

(b)longshore component

Fig.8 One hour averaged velocity measured in shallow water region

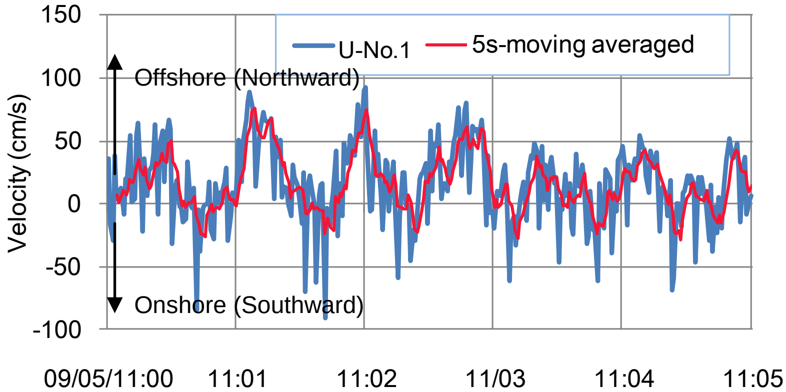

Fig.9 Measured raw velocity (cross-shore component) at No.1

(Sept.5, 11:00-11:05)

Figures 10 is the typical example of time history of the velocity vector at No.1 (Fig.(a)) and No.5 (Fig.(b)) depicted based on the 20s-moveing averaged current velocities in longshore and cross-shore components at 1s interval and the surface displacement measured by the pressure sensor at No.5 (Fig.(c)) on Sept.5, 11:00-11:03.

Again clear low frequency fluctuations of the period about 60s can be seen in the velocity vector and the same fluctuation appears in the water surface displacement as shown in Fig.10(c). The flow direction at No.1 fluctuates between NNW and NW and the flow direction at No.5 fluctuates between ESE and NE. On the other hand, the amplitude of the velocities at No.1 and No.5 are almost the same and they fluctuate between 40cm/s and 80cm/s. The amplitude of the mean surface displacement is about 10cm.

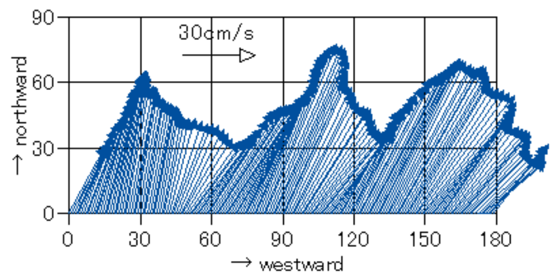

(a) Velocity vector at No.1 (Sept. 5, 10:42-10:45)

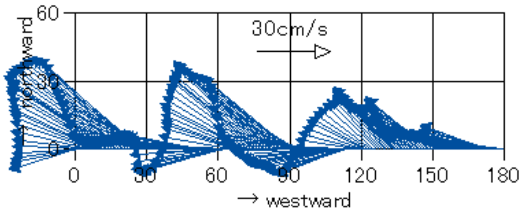

(b) Velocity vector at No.5 (Sept. 5, 10:42-10:45)

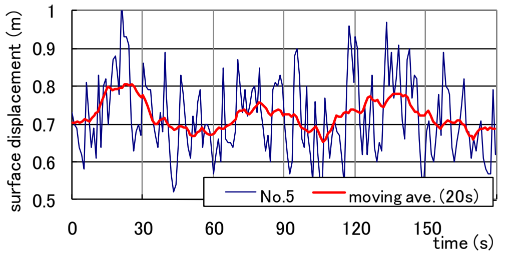

(c) Surface displacement at No.5 (Sept. 5,10:42-10:45)

Fig.10 Measured fluctuations in velocity vector and surface displacement (2007,09.05)

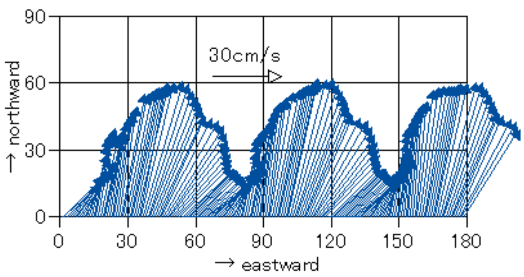

(a) Velocity vector at No.1

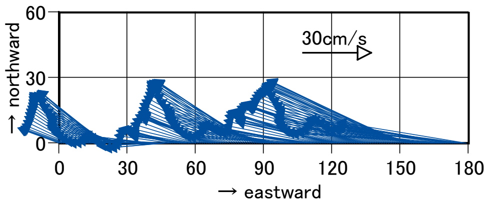

(b) Velocity vector at No.5

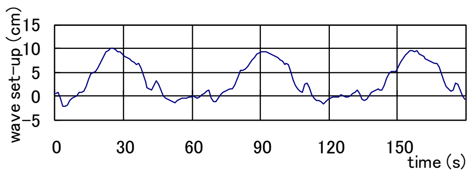

(c) Surface displacement at No.5

Fig.11 Calculated fluctuations in velocity vector and surface displacement (H_o =0.5m, T_l =60s, α =0/3, *T*=5s, θ=0deg.)

Investigation into the Cause of Low Frequency Fluctuations in the Shallow Water Region

The authors have already reported that these low frequency fluctuations are caused by the wave grouping of incident waves (Deguchi et al., 2008). Here, we would like to confirm that the low frequency fluctuations in surface displacement and wave-induced current in the decaying process of rip channel are caused by the intrinsic fluctuations of incident waves through numerical simulations.

Two kinds of sinusoidal low frequency fluctuations are assumed. One is the fluctuation in wave height H (wave grouping) and the other is the incident wave angle θ as follows;

$$H = H_o\left\{1+\alpha\sin\left(\frac{2\pi}{T_l}t\right)\right\} \qquad (1)$$

$$\theta = \theta_o\left\{1+\beta\sin\left(\frac{2\pi}{T_d}t\right)\right\} \qquad (2)$$

where H_o and θ_o are the mean wave height and direction, α and β are the amplitudes of low frequency fluctuations in wave height and direction, T_l and T_d are the period of low frequency fluctuations and T is the incident wave period.

Wave and wave-induced current are calculated by giving incident waves with low frequency fluctuation as expresses by Eq.1 and 2 at offshore boundary. To be more precise, waves and wave-induced current are calculated iteratively at time interval of 1/8 of the low frequency period until the stable solution is obtained. The calculation region was 100m (cross-shore direction)*300m (longshore direction) around the sensor array on the bottom measured on Sept.5 and the grid size was 0.5m in the both cross-shore and longshore directions. The depth at offshore boundary was about 2m. Wave transformation and wave-induced current are calculated by solving an unsteady mild slope equation and a so-called depth averaged shallow water equations numerically.

Figure 11 is the time fluctuations of velocity vector at No.1 (Fig.(a)) and No.5 (Fig.(b)) and surface displacement at No.5 (Fig.(c)) obtained after calculation of 5-cycle of low frequency motion where the calculated result was almost stable. Incident waves at offshore boundary was given by Eq. 1 (H_o =0.5m, T_l =60s, α =0/3, τ=5s, θ=0deg.).

The calculated fluctuations of velocity vectors at No.1 and No.5 (Figs.11 (a) and (b)) agree with measured results (Fig.11 (a) and (b)) moderately. Further, the amplitude of calculated surface displacement (Fig.11 (c)) is about 10cm and this value of the amplitude reproduces the measured one.

Figure 12 is the calculated velocity vector around sensor array at the end of 8-cycle of low frequency motion which corresponds to 180s of the horizontal axis in Figs. 10 and 11. A clear clockwise circulation appears. The circulation shifts its location according to the phase of the low frequency fluctuation of the incident waves and this is the reason for the large spatial gradient of the measured current velocity. Figure 13 is the snap shot of the video image recorded at 11am on Sept.5. The green color is the sea marker we used as tracer and a clear clockwise circulation just same as the calculated circulation is observed.

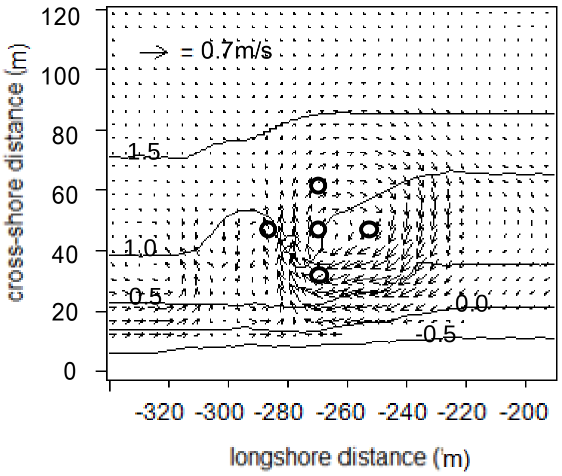

Fig.12 Calculated flow pattern of wave-induced current around the sensor array (2007,09.05)

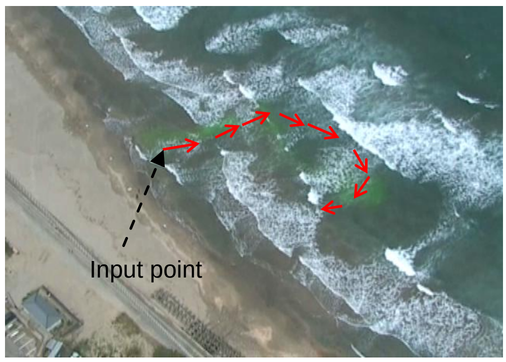

Fig.13 Snap shot of the video image recorded at 11am on Sept.5

It is confirmed that fluctuation in incident wave direction also causes another fluctuation in the wave-induced current numerically.

EARLY STAGE OF THE DEVELOPMENT OF RIP CHANNEL

In 2009, we started field measurements on Sept 4. At that time there was no characteristic profile on the bottom topography. Therefore, we put five sets of sensors on line at 5m interval on the place where rip channel might be generated.

Measured Bottom Topography in the Fading Process of Rip Channel

Figure 13 illustrates the measured bottom topography during field observation in 2009. Until Sept 7 there was not any significant change in bottom profile. However, wave height suddenly increased from the noon of Sept 8 and rip current was generated just on our sensors. The water depth around the sensors begun to increase and finally a rip channel appeared on Sept 10. At the same time longshore bar was formed in the west of the sensor array.

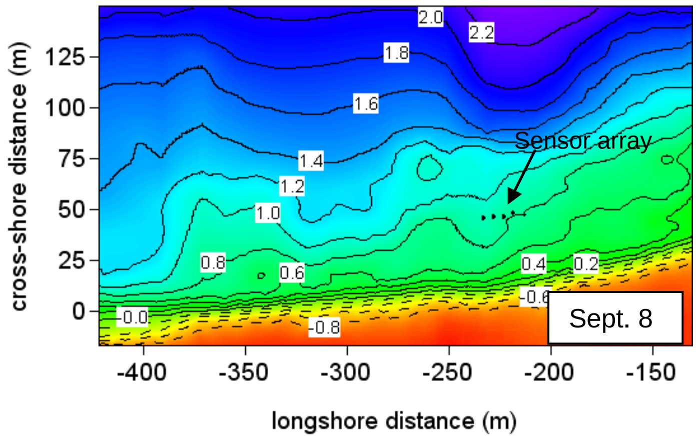

(b) September 8

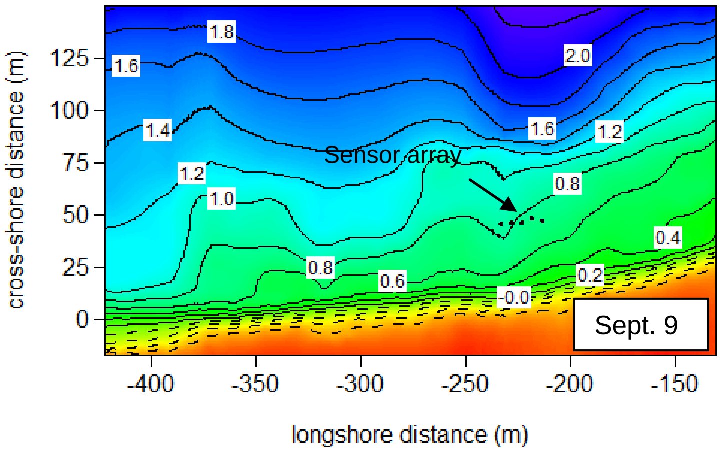

(b) September 9

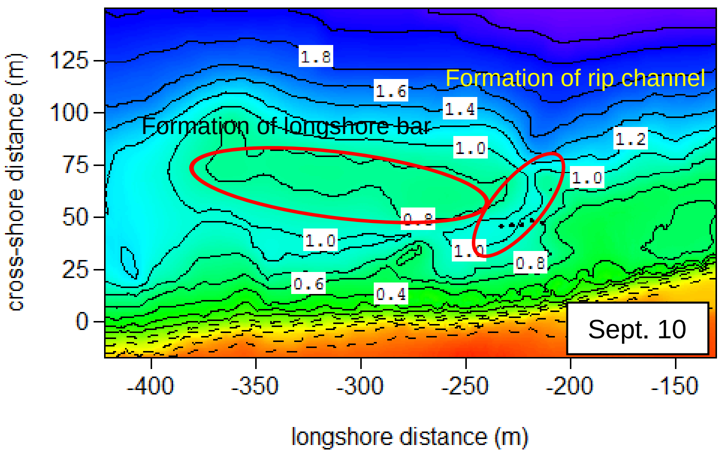

(c) September 10

Fig.14 Measured bottom topography in Sept. 2009

Incident Waves during Field Observation

Figure 15 is the significant wave height and period measured at the depth of about 8m (No.0; Fig.(a)) and the wave direction at No.0 and Nos. 1 and 4 in the shallow water region (Fig.(b) and the significant wave height at Nos.1 and 4 (Fig.(c)). The upper right figure in Fig.15 (b) and (c) is the arrangement of sensor array.

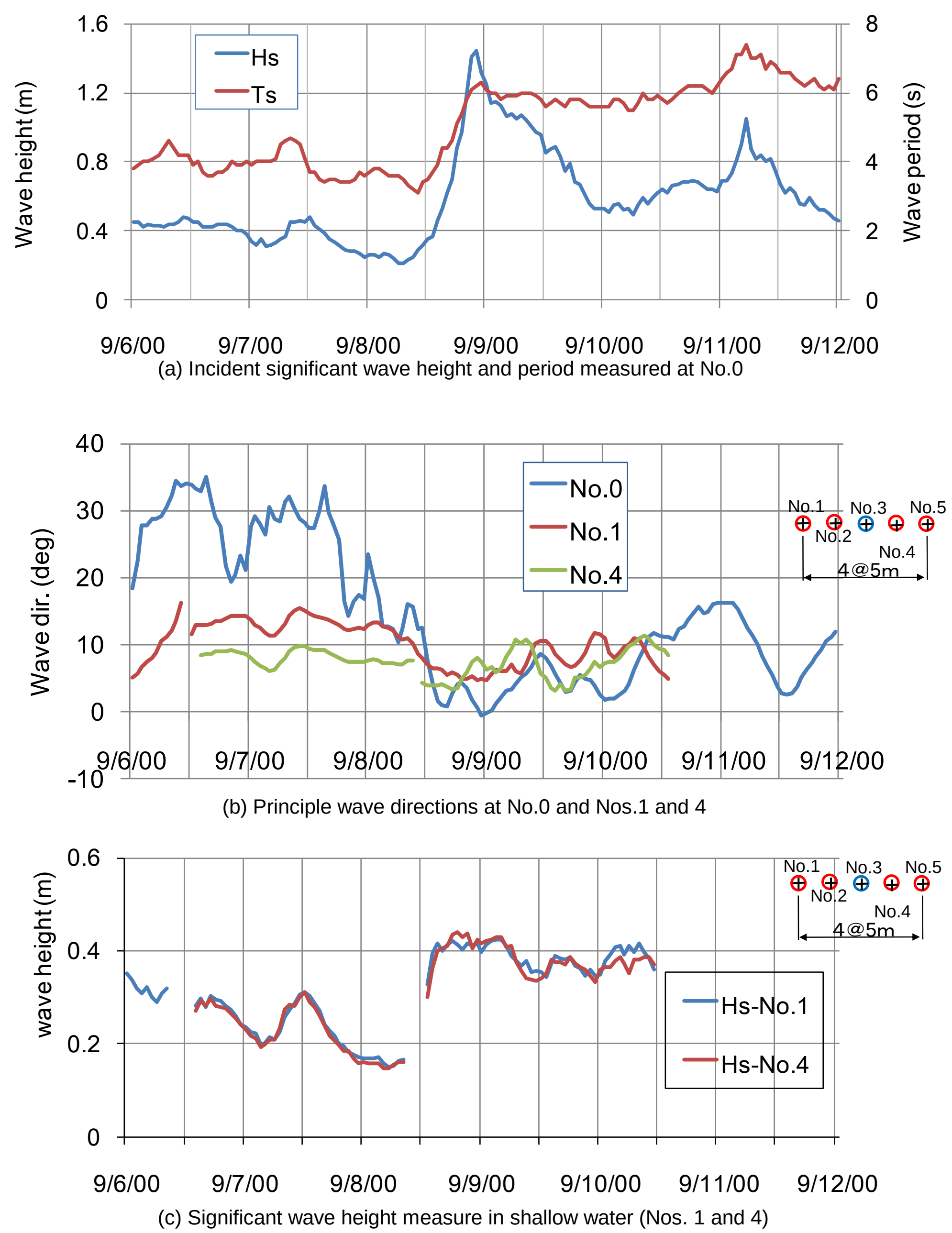

Fig. 15 Incident significant wave height and period measured at No.0

Wave height increased rapidly from the morning of Sept8 and wave direction changed from NNE to N according to the increase in wave height. The distance between No.1 and No.4 was about 15m. From Fig. 15(c), it is found that a relatively uniform wave transformation took place during this period.

Measured Current Velocity in Shallow Water Region

Figure 16 illustrates the one hour time averaged cross-shore component (Fig.(a)) and longshore component (Fig.(b)) of the measured current velocities and the maximum offshore velocity of the 20s-moving averaged velocity (Fig.(c) at No.1 and No.4. Again the upper right figure in these figure is the sensor array.

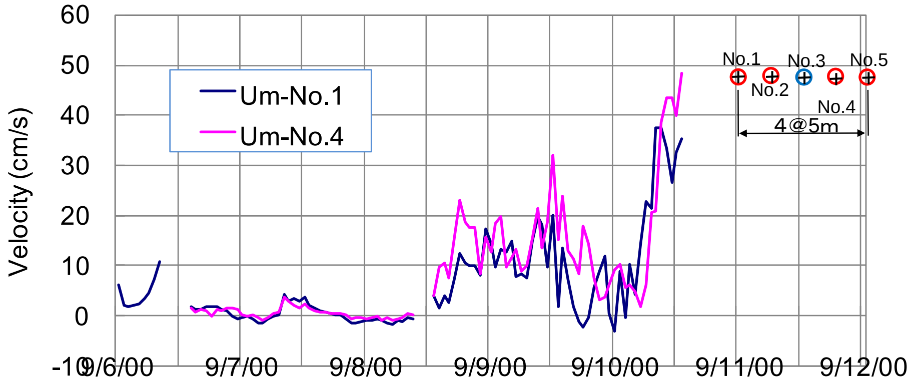

(a)One hour averaged velocity of cross-shore component

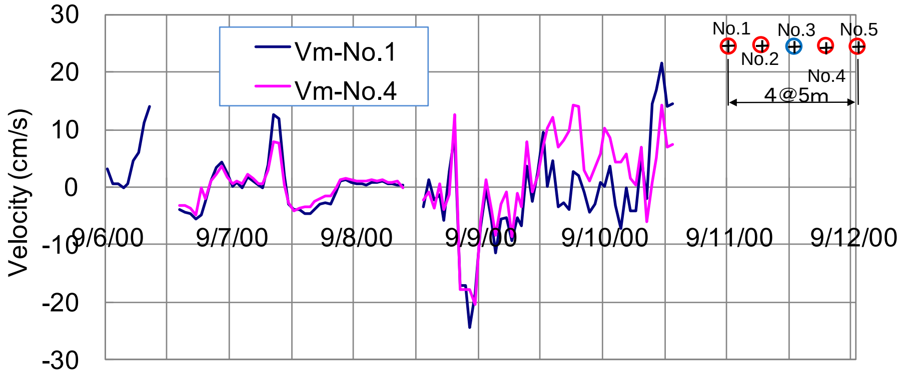

(b) One hour averaged velocity of longshore component

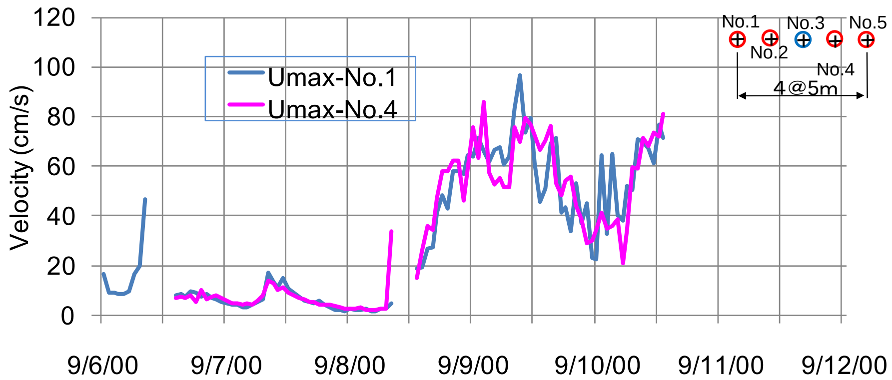

(c) Maximum offshore velocity of 20s-moving averaged velocity

Fig.16 Maximum offshore velocity of 20s-moving averaged velocity

It can be seen that no significant current was generated until the incident wave height increased. Just after the sudden increase in the incident waves, a rip current broke out. High waves continued for only 12hours. During this period, the depth of the path of rip current became deep. Although the rip current lost impetus at one point according to the decrease in wave height, it kept up the offshore momentum. In the mean time, further erosion along the rip current continued and the depth became deep that added further impetus for the rip current. Two days after the generation of rip current, the maximum value of the 20s-moving average rip current velocity reached 80cm/s again and the one hour averaged offshore velocity became more than 40cm/s. This result suggests that a positive feedback exists between the rip current and formation of rip channel.

These strong current together with high wave begun to transport sediment near the sensors and rip channel was generated. As a result, the water depth at the sensor became 0.3-0.4m deeper than the initial water depth. We knocked off our measurement in the afternoon of Sept. 10 for the sake of our safety because of the strong rip current.

Estimated Flow Pattern in the Formation Process of Rip Channel

To investigate the reason for the break out of rip current on Sept.8 and the growth of rip current after Sept.9 numerical simulations were conducted on the bottoms measured on Sept.8, 9 and 10. The results are shown in Fig.17.

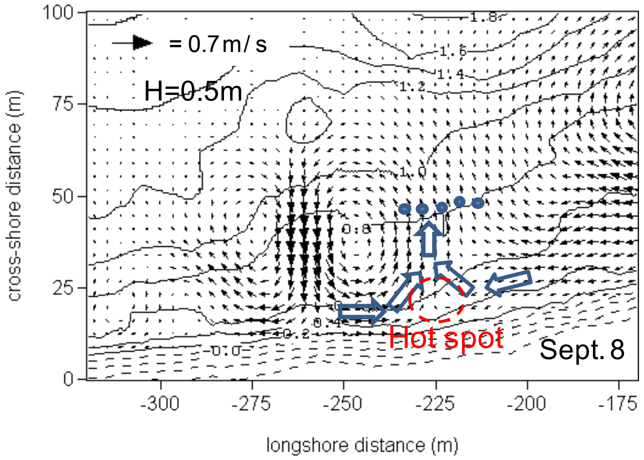

(a)Calculated flow pattern on the bottom profile measured on Sept.8

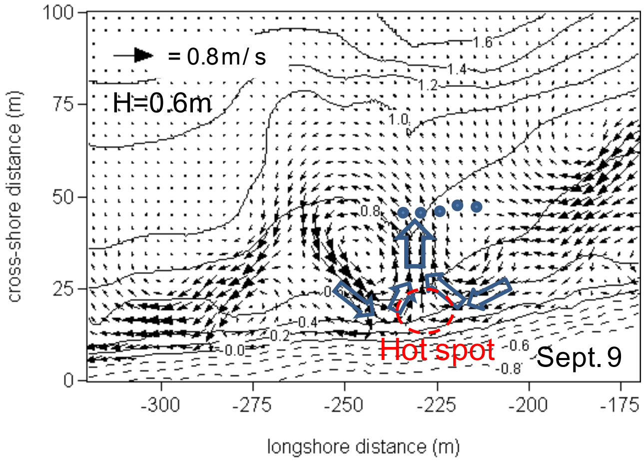

(b)Calculated flow pattern on the bottom profile measured on Sept.9

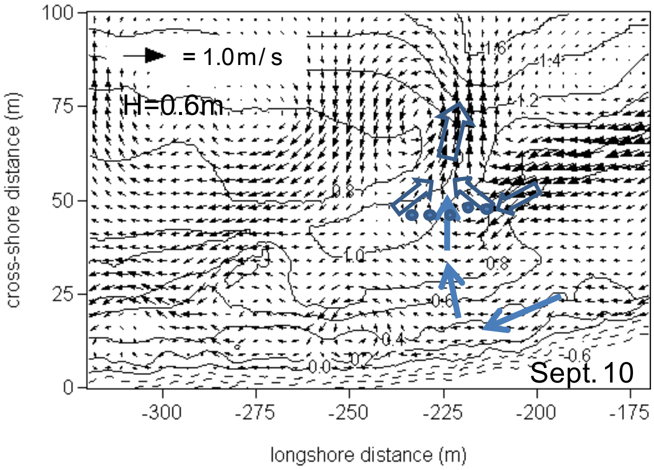

(c)Calculated flow pattern on the bottom profile measured on Sept.10

Fig.17 Calculated flow pattern of wave-induced current

After the wave height increased, a hot spot where longshore currents converge is generated and rip current appears just on our sensors (Fig.17 (a)). This current eroded the bottom along the flow. On the bottom topography of Sept 9, the hot spot became clearer and erosion was getting on (Fig.17 (b)). After the formation of rip channel, strong rip current was generated even when the incident wave height decreased (Fig.17 (c)). From these results, it is judged that the formation of the hot spot and/or convergence of longshore current acts as a trigger of the generation of rip current in this case.

Figure 18 is a snap shot of the video image recorded in the morning of Sept.10. Red circles are the ground control points and the distance between GCP-A1 andGCP-A4 was 71.5m. The sea-marker thrown into the sea first diverged in the longshore direction from the input point and then flowed toward offshore. Later on, the sea-marker smashed through breaker zone and flowed far offshore.

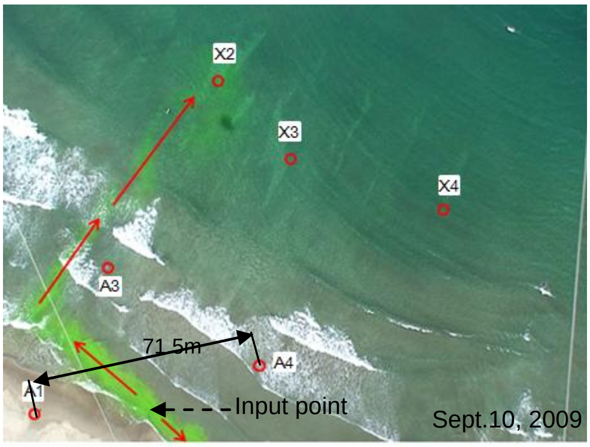

Fig.18 Snap shot of the video image recorded in the morning of Sept. 10

On Sept. 9, a relatively strong rip current existed. However, the sea-marker could not flow out of the breaker zone because of high waves and wide breaker zone. Rip current began to flow out of breaker zone after the incident wave height decreased.

CONCLUSIONS

Disappearance and formation processes of rip channel are discussed through the field observations of wave, nearshore current and topography change. The source of the low frequency fluctuations of the period few minutes in near shore current is also investigated based on the measured results. The main results obtained in this study are summarized as follows:

Formation of the hot spot and/or the convergence of longshore current act as a trigger of the generation of rip current.

The fluctuations with time scale of few minutes in nearshore current are caused by the intrinsic fluctuation of the incident waves and have nothing to do with the topography change such as the creation of rip channel and disappearance of rip channel.

Significant change in the incident wave characteristics took place during few hours is responsible for the generation and annihilation of rip channel through the interaction between wave transformation, wave-induced current and topography change.

ACKNOWLEDGMENTS

A part of this study was supported by Grant-in-Aid for Scientific Research (B), 20360221, JSPS. Further support has been given by Japan Coast Guard in the field works.

REFERENCES

Arita M., I. Deguchi and H. Yabusaki, 2007. Experimental study on estimation of bottom topography through video images, *Proceedings of the 3rd International Conference on Asian and Pacific Coast, 2007*, Nanjing, China

Deguchi, I. and S. Araki, 2006. Characteristics of rip current on large cusps, *Proceedings of 30th International Conference on Coastal Engineering*, ASCE, 1135-1145
Nowphas, 2007. http://www.mlit.go.jp/kowan/nowphas/